Environmental impacts of polarity-resolved water-soluble organic matter from animal dung burning on the Qinghai-Tibet Plateau

Shasha Huang[1], Zhenxing Shen[1*], Cailan Li[1], He Shen[1], Yaling Zeng[2], Liu Yang[1], Jian Sun[1], Hongmei Xu[1]

[1] *Department of Environmental Sciences and Engineering, Xi'an Jiaotong University, Xi'an, 710049, China*

[2] *School of Environmental Science and Engineering, Southern University of Science and Technology, 518055, Shenzhen, China*

*Author to w*hom correspondence should be addressed.*

E-mail: zxshen@mail.xjtu.edu.cn (Zhenxing Shen)

Contents of this file

Text S1. Separation of three types of WSOM

Three types of WSOM were separated using a multi-step solid phase extraction procedure with Oasis hydrophilic-lipophilic balance (HLB) column (3 cc, 60 mg). The detailed extraction production can be found in previous studies (Chen et al., 2016a; Chen et al., 2016b; Mukherjee et al., 2020; Zhang et al., 2022c). Briefly, a quartz filter membrane with a certain area to collect $PM_{2.5}$ was used for ultrasonic extraction with 6 mL ultra-pure water for 30 min, and then filtered with a 0.45μm Teflon syringe to collect filtrate, namely WSOM. The pH of WSOM was adjusted to 7 with 0.01 M NaOH, passed through an HLB column (60 mg), and the residual solution was washed with 1 mL of deionized water. HULIS-n was obtained by eluting the adsorbent with 2 mL methanol solution containing 2% ammonia, the extract was completely dried with nitrogen stream and redissolved with 1 mL ultra-pure water. The effluent from the previous step was collected and the pH was adjusted to 2 with 1 M HCl. It was passed through another pre-activated HLB column followed by the addition of 1 ml of 0.01 M HCl to the column. The adsorbed material on the column was eluted with 2 ml methanol to obtain HULIS-a. The waste water from the previous step is collected in a glass bottle. Due to the adsorption mechanism of the HLB column, this component contains high levels of polar substances and is known as HP-WSOM. Freeze dry and dissolve in 1ml ultra-pure water.

Reference

Chen, Q., Ikemori, F., Higo, H., Asakawa, D., Mochida, M., 2016a. Chemical Structural Characteristics of HULIS and Other Fractionated Organic Matter in Urban Aerosols: Results from Mass Spectral and FT-IR Analysis. Environmental Science & Technology 50, 1721-1730.

Chen, Q., Ikemori, F., Mochida, M., 2016b. Light Absorption and Excitation-Emission Fluorescence of Urban Organic Aerosol Components and Their Relationship to Chemical Structure. Environmental Science & Technology 50, 10859-10868.

Mukherjee, A., Dey, S., Rana, A., Jia, S., Banerjee, S., Sarkar, S., 2020. Sources and atmospheric processing of brown carbon and HULIS in the Indo-Gangetic Plain: Insights from compositional analysis. Environ Pollut 267, 115440.

Zhang, T., Shen, Z.X., Huang, S.S., Lei, Y.L., Zeng, Y.L., Sun, J., Zhang, Q., Ho, S.S.H., Xu, H.M., Cao, J.J., 2022c. Optical properties, molecular characterizations, and oxidative potentials of different polarity levels of water-soluble organic matters in winter $PM_{2.5}$ in six China's megacities. Sci. Total Environ. 853.

Text S2. Calculation of light absorption and radiative forcing

The coefficients characterizing the absorption characteristics of the three types of WSOM are calculated as follows:

$$b_{abs-\lambda} = (A_\lambda - A_{700}) \times \frac{V_1}{V_a \times L} \times \ln(10), \quad (1)$$

$$EF\ of\ b_{abs-\lambda} = \frac{b_{abs-\lambda}}{m}, \quad (2)$$

where A_{700} is the absorbance of the sample at 700 nm, which is used to correct the baseline deviation, V_1 is the ultrapure water used to extract the sample, V_a is the atmospheric sampling volume corresponding to the sample, L is the optical path length of the cuvette (1 m), m is the mass of fuel (kg), and K is a constant.

The mass absorption efficiency at 365 nm (MAE_{365}) can be used to characterize the light absorption capacity of three types of WSOM:

$$MAE_\lambda = \frac{b_{abs-\lambda}}{C_{HULIS}} \quad (3)$$

where $b_{abs\text{-}\lambda}$ is the absorption coefficient of the corresponding wavelength and C_{HULIS} is the concentration of three WSOM (μg/m^3).

Simple forcing efficiency (SFE, W/g) represents the energy per unit mass of aerosol species perturbed by the atmosphere (Bond and Bergstrom, 2006; Choudhary et al., 2021; Lei et al., 2018). The SFE calculation process for the three types of WSOM is as follows:

$$\frac{dSFE_{WSOM}}{d\lambda} = -\frac{1}{4}\frac{dS(\lambda)}{d\lambda}\tau_{atm}^2(1-F_c)\cdot\left[2(1-a_s)^2\beta(\lambda)\cdot MSE_p(\lambda) - 4a_s\cdot MAE_p(\lambda)\right] \quad (4)$$

Where $\frac{dS(\lambda)}{d\lambda}$ represents the solar spectral irradiance (W/m^2/nm) retrieved in the Air Mass 1 Global Horizon (AM1GH) solar irradiance model (Levinson et al., 2010), τ_{atm} is the atmospheric transmittance of 0.79, F_c is the cloud fraction of 0.6, α_s is the surface albedo of 0.19, β is the backward scattering fraction, and MSE_p and MAE_p represent the scattering and absorption efficiency per unit mass of the measured aerosol particles, respectively, in m^2/g (Nakayama et al., 2013; Peng et al., 2022). $\beta(\lambda)$ is the backscattering fraction estimated using the quadratic polynomial:

$$\beta = 0.0817 + 1.8495b - 2.9682b^2 \quad (5)$$

$$b = \frac{1-g^2}{2g}\left[\frac{1}{\sqrt{1+g^2}} - \frac{1}{1+g}\right] \quad (6)$$

Where g and b are referred to as the asymmetric parameter and the ratio of the backscattering coefficient to the total scattering coefficient, respectively.

In this study, considering only absorption, we performed Mie calculations at 280-700 nm and 280-400 nm every 1 nm to provide MAE, thus simplifying Eq. (5) to:

$$\frac{dSFE_{WSOM}}{d\lambda} = \frac{dS(\lambda)}{d\lambda}\tau_{atm}^{2}(1 - F_c)\cdot\left[a_s \cdot MAE_p(\lambda)\right] \quad (7)$$

Reference

Bond, T.C., Bergstrom, R.W., 2006. Light absorption by carbonaceous particles: An investigative review. Aerosol Science And Technology 40, 27-67.

Choudhary, V., Rajput, P., Gupta, T., 2021. Absorption properties and forcing efficiency of light-absorbing water-soluble organic aerosols: Seasonal and spatial variability. Environ. Pollut. 272.

Lei, Y.L., Shen, Z.X., Zhang, T., Zhang, Q., Wang, Q.Y., Sun, J., Gong, X.S., Cao, J.J., Xu, H.M., Liu, S.X., Yang, L., 2018. Optical source profiles of brown carbon in size-resolved particulate matter from typical domestic biofuel burning over Guanzhong Plain, China. Sci. Total Environ. 622, 244-251.

Levinson, R., Akbari, H., Berdahl, P., 2010. Measuring solar reflectance-Part I: Defining a metric that accurately predicts solar heat gain. Solar Energy 84, 1717-1744.

Nakayama, T., Sato, K., Matsumi, Y., Imamura, T., Yamazaki, A., Uchiyama, A., 2013. Wavelength and NOx dependent complex refractive index of SOAs generated from the photooxidation of toluene. Atmos. Chem. Phys. 13, 531-545.

Peng, H.Y., Wang, Y.S., Wang, Y.L., Chen, Y.K., Li, D., Xue, H., 2022. Characteristics of emission and light-absorption of size-segregated carbonaceous aerosol emitted from four types of coal combustion at different combustion temperatures. Atmos. Pollut. Res. 13.

Table S1. Uncertainty ranges and coefficients of variation for different pollutants in emission estimates.

Pollutant	Uncertainty
HULIS-n	-52.9%-303%
HULIS-a	-65.7%-319%
HP-WSOM	-54.7%-290%

Table S2. The EF, MAE_{365}, EF of $b_{abs\text{-}365}$ and EF of OP of HULIS-n, HULIS-a, and HP-WSOM from coal heating and cooking combustion.

Sample	Coal for heating				Coal for cooking			
	EF	MAE_{365}	EF of $b_{abs\text{-}365}$	EF of OP	EF	MAE_{365}	EF of $b_{abs\text{-}365}$	EF of OP
	g/kg	m^2/g	m^2/kg	$(AU\ s^{-1}g^{-1})/kg$	g/kg	m^2/g	m^2/kg	$(AU\ s^{-1}g^{-1})/kg$
HULIS-n	0.34±0.14	1.69±0.07	22.43±11.42	0.12±0.04	0.17±0.18	1.94±1.18	8.95±5.56	0.16±0.11
HULIS-a	0.51±0.39	0.80±0.15	14.66±9.82	0.04±0.01	0.11±0.09	4.17±3.38	11.57±1.07	0.23±0.21
HP-WSOM	0.05±0.03	6.12±0.74	11.87±9.42	0.54±0.13	0.03±0.01	5.59±0.52	6.94±1.21	0.41±0.05

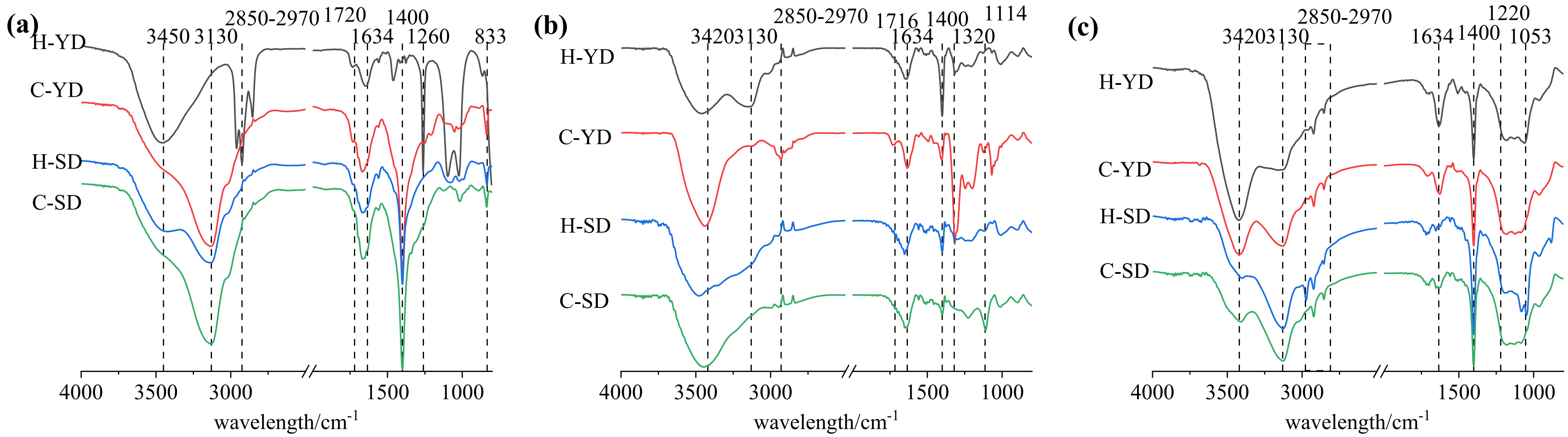

Figure S1. The FT-IR spectra of HULIS-n (a), HULIS-a (b), and HP-WSOM (c) produced by the combustion of yak dung and sheep dung.

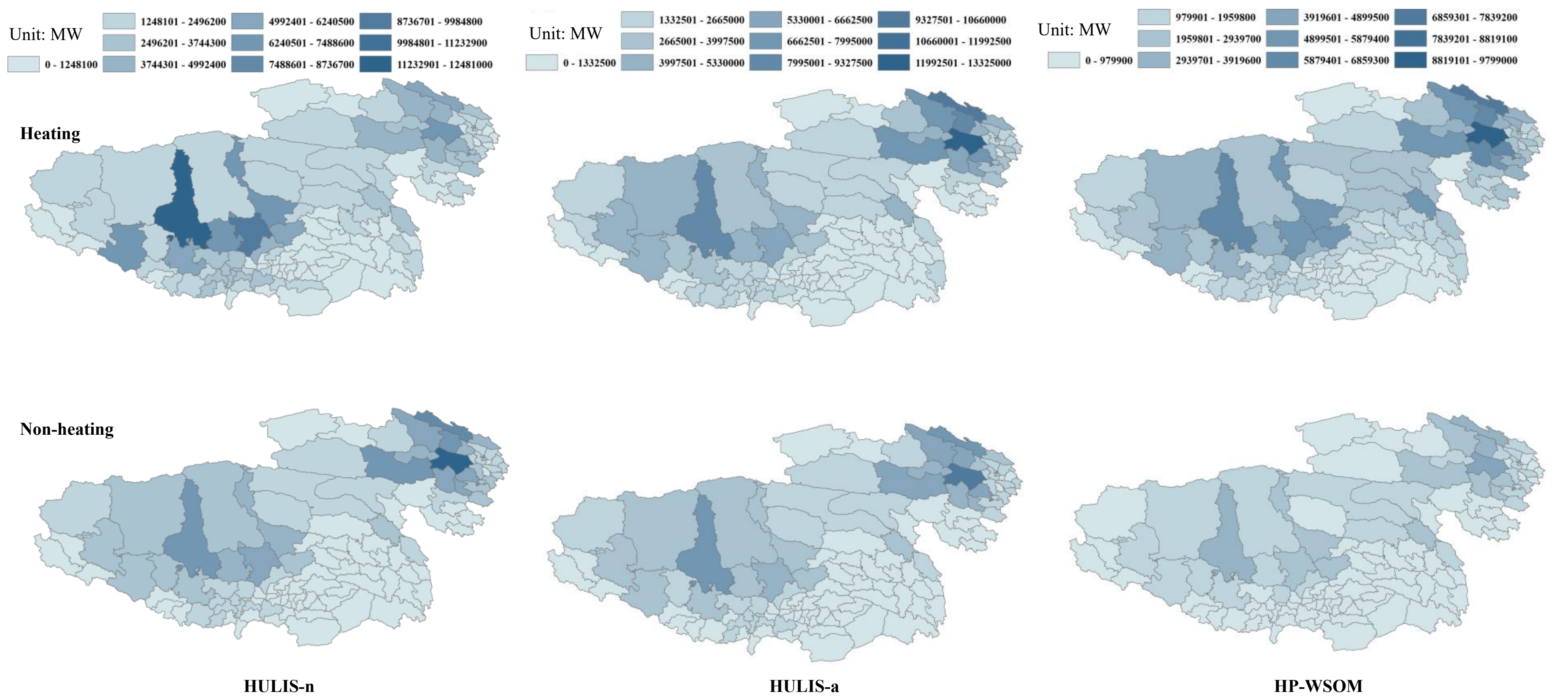

Figure S2. The radiation effects of HULIS-n, HULIS-a and HP-WSOM in the range of 280-700 nm from the burning of yak dung and sheep dung on the QTP.

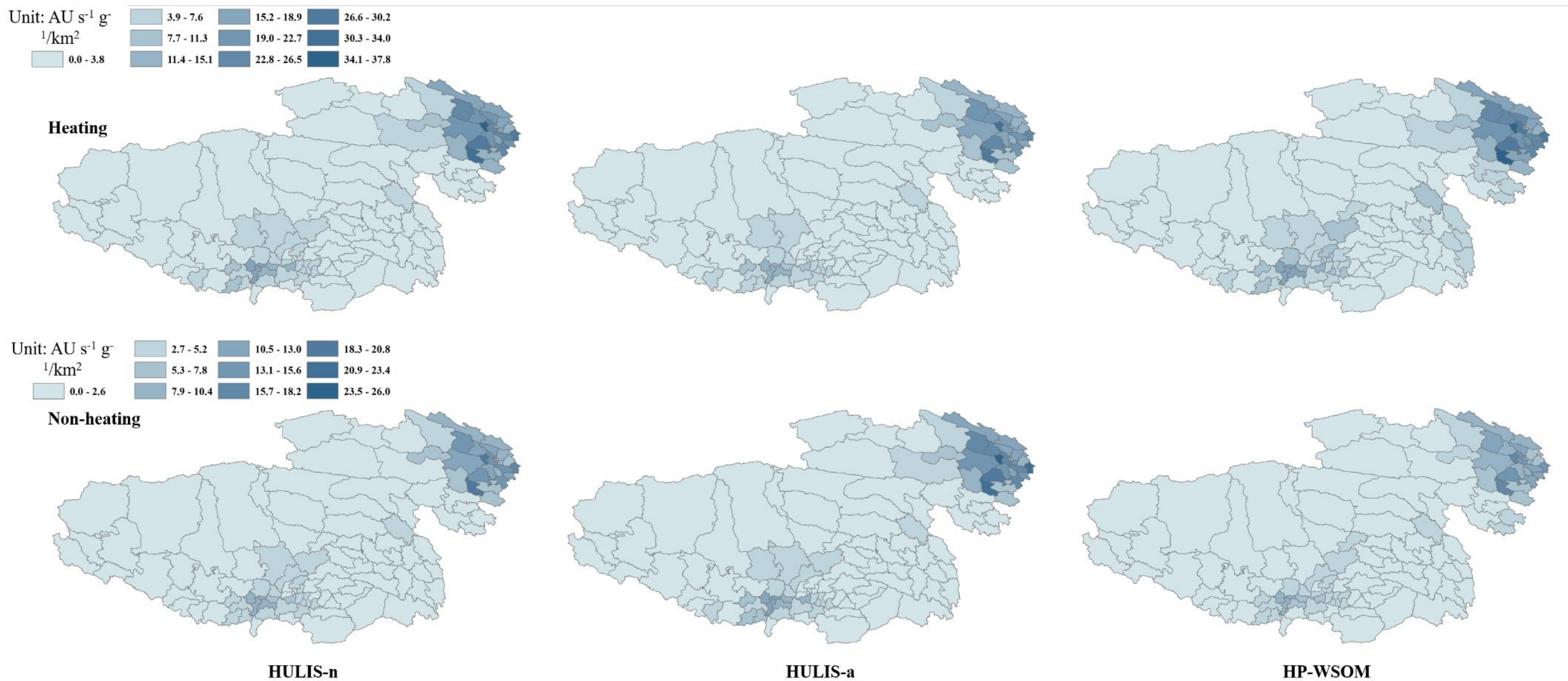

Figure S3. The oxidation potential density of HULIS-n, HULIS-a and HP-WSOM from yak dung and sheep dung burning on the QTP.